

# Simulation of Fixed-Bed Adsorption for Biogas Upgrading



Lucas F. A. S. Zafanelli, Ezzeldin Aly, Adriano Henrique, Alírio E. Rodrigues, and José A. C. Silva

## 1 Introduction

Great efforts have been devoted to developing clean energy sources of energy that can contribute to keeping global warming below 2 °C in the incoming 30 years. Global warming is mainly caused by the emission of anthropogenic greenhouse gas such as methane (CH<sub>4</sub>) and carbon dioxide (CO<sub>2</sub>), being CH<sub>4</sub> almost 28 times more damaging than CO<sub>2</sub> [4]. Biogas is a sustainable and renewable source of energy mainly composed of CH<sub>4</sub> and CO<sub>2</sub> and low levels of N<sub>2</sub> [2, 8]. In this way, producing biogas and upgrading it to biomethane is an alternative solution to prevent greenhouse gas emissions at the same time it can be supplied as a renewable source of biofuel. Furthermore, biogas can be a decentralized alternative to produce clean energy everywhere, as it is easily produced from the methanation of biomass and organic wastes from sewage sludge anaerobic digestion, commercial composting, landfills, biomass gasification (thermo-chemical production process), animal farm manure anaerobic

---

L. F. A. S. Zafanelli (✉) · E. Aly · A. Henrique · J. A. C. Silva  
Centro de Investigação de Montanha (CIMO), Instituto Politécnico de Bragança, Campus Santa Apolónia, 5300-253 Bragança, Portugal  
e-mail: [zafanelli@ipb.pt](mailto:zafanelli@ipb.pt)

Laboratório Associado Para a Sustentabilidade E Tecnologia Em Regiões de Montanha (SusTEC), Instituto Politécnico de Bragança, Campus de Santa Apolónia, 5300-253 Bragança, Portugal

L. F. A. S. Zafanelli · A. Henrique · A. E. Rodrigues  
Laboratory of Separation and Reaction Engineering (LSRE), Associate Laboratory LSRE/LCM, Department of Chemical Engineering, Faculty of Engineering, University of Porto, 4099-002 Porto, Portugal

E. Aly  
Faculdade de Engenharia, Associate Laboratory in Chemical Engineering (ALiCE), Universidade do Porto, Rua Dr. Roberto Frias, 4200-465 Porto, Portugal

co-digestion with energy crops, agro-food industry digestion facilities [2], among others.

The presence of  $\text{CO}_2$  (up to 40 vol. %) and  $\text{N}_2$  (up to 15 vol.%) in the biogas composition (landfill gas), reduces its calorific value and causes corrosion of engines and pipelines, limiting its use and transportation via natural gas pipelines [2]. Accordingly, biogas needs to be upgraded (by removing  $\text{CO}_2$  and  $\text{N}_2$ ) to obtain biomethane that can be either injected into natural gas grids or directly used as a vehicle/domestic fuel. However, to use biomethane as a vehicle fuel or to inject it into natural gas pipelines, standard requirements must be followed depending on country rules. For example, the methane content in Switzerland must be  $\geq 96$  vol%, and only  $\geq 86$  vol% in France. In these two countries, the  $\text{CO}_2$  content is also different, being  $\leq 4$  (Switzerland) and  $\leq 2.5$  vol% (France) [2].

To meet the standard requirements for biogas upgrading the main separation techniques reported in the literature can be water or organic solvent scrubbing, chemical absorption, adsorption, cryogenic separation, membrane technology, biological upgrading, and in-situ upgrading methods [2, 5, 6]. Among them, adsorption processes such as Pressure/Vacuum or Temperature Swing Adsorption (PSA/VSA or TSA) have been employed, being very competitive with low energy consumption. At the same time, a variety of solid adsorbents are already available or will be developed in the future to increase the performance of the adsorption processes [6, 8, 16]. Moreover, several operating parameters namely pressure, flow rates, temperatures, different cycle steps (e.g. pressurization, feed-high pressure, blow-down/depressurization, equalization, backfill, low-pressure purge, etc.), and their tuning should be optimized to provide efficient performance in the biogas upgrading. Thus, mathematical modeling is a fundamental tool for the design of adsorption processes allowing us to evaluate the effect of several operating parameters to find the best-operating conditions, besides significantly reducing the number of experiments required.

In this work, an adsorption simulation package to study the separation of the main components of biogas ( $\text{CO}_2/\text{CH}_4/\text{N}_2$ ) in a fixed bed was developed and validated by predicting experimental single and ternary breakthrough curves on binder-free zeolite 4A and KY. Overall, the simulator proved to be very efficient to predict the fixed-bed experimental data adsorption dynamics, and it has now been used in the simulation and design of more complex systems like PSA/VSA to TSA processes for biogas upgrading at the industrial level with proper boundary conditions.

## 2 Materials and Methods

### 2.1 Materials

In this work, two types of benchmark zeolites were studied, namely, potassium exchanged (95%) type Y (BFKY) and sodium type A (BF4A). These zeolites were synthesized and transformed into beads through the binder-free method [10, 11] by Chemiewerk Bas Köstritz GmbH (Germany). The adsorbent bead's particle diameter ranges from 1.6 to 2.5 mm. He (99.9998%), CO<sub>2</sub> (99.998%), CH<sub>4</sub> (99.95%), and N<sub>2</sub> (99.999%) were supplied by Air Liquide.

### 2.2 Experimental Procedure

A homemade fixed-bed adsorption apparatus has been used to collect the breakthrough curves of CO<sub>2</sub>, CH<sub>4</sub>, and N<sub>2</sub> and their binary/ternary mixtures which were used to validate the adsorption mathematical model simulation package. This apparatus has been used in our previous work [15], where detailed information on its layout can be found. In the adsorption studies, a stainless steel adsorption column (0.0286 m i.d. and 0.0646 m length) has been used. For the experiments, the column was filled with 23.8 g of BF4A and 26.2 g of BFKY, which leads to a bulk density of 590 and 649 kg m<sup>-3</sup>, respectively.

### 2.3 Mathematical Model

The adsorption mathematical model and respective boundary conditions for fixed-bed adsorption are shown in Table 1 and were derived according to the following assumptions: (i) the gas is considered to follow the ideal gas law; (ii) an axially dispersed plug flow model is used to represent the bulk fluid flow through the bed; (iii) constant bulk density in the bed; (iv) the pressure drop is negligible; (v) the radial gradients of concentration, temperature, and pressure are negligible; and (vi) the adsorption equilibrium is described by the extended dual-site Langmuir isotherm model (DSL). Moreover, it was considered a column of length  $L$ , void fraction  $\varepsilon_b$  ( $=0.4$ ), packed with a solid adsorbent through which an ideal biogas stream (mainly CH<sub>4</sub>/CO<sub>2</sub>/N<sub>2</sub>) flows at a molar flow rate  $F$ , where  $C$  is the total gas concentration of the species in the mixture,  $y_i$  represent the molar fraction of adsorbable species  $i$  in the fluid, and  $\bar{q}_i$  the average adsorbed concentration of adsorbable species  $i$  in the adsorbent solid phase.

**Table 1** Fixed-bed adsorption mathematical model equations

Model	Equations	
Ideal gas	$C = \frac{P}{RT}$	(1)
Overall mass balance	$\frac{\partial F}{\partial z} + \varepsilon_b \frac{\partial C}{\partial t} + \rho_p (1 - \varepsilon_b) \sum_{i=1}^n \frac{\partial \bar{q}_i}{\partial t} = 0$	(2)
Component mass balance	$-\varepsilon_b D_{ax} \frac{\partial}{\partial z} \left( C \frac{\partial y_i}{\partial z} \right) + \frac{\partial (F y_i)}{\partial z} + \varepsilon_b \frac{\partial (C y_i)}{\partial t} + \rho_p (1 - \varepsilon_b) \frac{\partial \bar{q}_i}{\partial t} = 0$	(3)
Mass transfer rate	$\frac{\partial \bar{q}_i}{\partial t} = K_{LDF} (q^* - \bar{q}_i)$	(4)
Linear Driving Force (LDF)	$\frac{1}{K_{LDF}} = \frac{R_p}{3k_f} + \frac{R_p^2}{15\varepsilon_p D_p} + \frac{r_c^2}{15K D_c}$	(5)
Gas-phase energy balance	$-K_{ax} \frac{\partial^2 T}{\partial z^2} + F c_{pg} \frac{\partial T}{\partial z} + C \varepsilon_b C_{pg} \frac{\partial T}{\partial t} + (1 - \varepsilon_b) a_p h_p (T - T_s) + a_c h_w (T - T_w) = 0$	(6)
Solid-phase energy balance	$C_{ps} \frac{\partial T_s}{\partial t} = a_p h_p (T - T_s) + \rho_p \sum_{i=1}^n (-\Delta H_{st,i}) \frac{\partial \bar{q}_i}{\partial t}$	(7)
Isotherm model (DSL)	$q_i = \frac{q_{m1} b_{1i} p_i}{1 + \sum_{j=1}^n b_{1j} p_j} + \frac{q_{m2} b_{2i} p_i}{1 + \sum_{j=1}^n b_{2j} p_j}$	(8)
Boundary conditions	$z = 0 \begin{cases} F y_{if} = F y_i - \varepsilon_b D_{ax} C \frac{\partial y_i}{\partial z} \\ F c_{pg} T_f = F c_{pg} T - K_{ax} \frac{\partial T}{\partial z} \\ F = F_f \end{cases}$ $z = L \begin{cases} \frac{\partial y_i}{\partial z} = 0 \\ \frac{\partial T}{\partial z} = 0 \end{cases}$	(9)

## 2.4 Numerical Model

For the solution of the model, the method of the lines was applied to reduce the set of coupled partial and algebraic differential equations into a system of ordinary and algebraic differential equations [9]. The spatial coordinate was discretized by the orthogonal collocation method [14]. In the orthogonal collocation method, the collocation points which represent each spatial coordinate or node in the numerical grid are determined by using Jacobi polynomials,  $P_{N(\alpha,\beta)}(x)$ , with  $\alpha = 0$ ,  $\beta = 0$ , where  $N$  is the number of collocation points. The approximation of the first and second derivatives was made by collocation matrices routines  $A_{i,j}$  and  $B_{i,j}$ , respectively. Therefore, the reduced system of ordinary differential equations was solved using the integrator ode15s available in the MATLAB library [12], and the algebraic differential equations were solved by Gauss elimination described elsewhere [14]. The simulator shows satisfactory accuracy and stability by using 25 spatial collocation points.

### 3 Results and Discussion

#### 3.1 Equilibrium of Adsorption

The adsorption equilibrium data of CO<sub>2</sub>, CH<sub>4</sub>, and N<sub>2</sub> in BF4A and BFKY were collected at 313 K and partial pressures up to 3.5 bar by fixed-bed breakthrough experiments described in a previous work [1, 15]. Figure 1 shows the isotherms collected for CO<sub>2</sub>, CH<sub>4</sub>, and N<sub>2</sub> together with the standard Langmuir (for CH<sub>4</sub> and N<sub>2</sub>) and dual-site Langmuir (DSL for CO<sub>2</sub>) isotherm models fittings (lines), for BF4A (open symbols) and BFKY (closed symbols) at 313 K.

From Fig. 1, it is possible to see that, as the pressure increases, the amount adsorbed of all components increases, which means that the equilibrium data is thermodynamic consistent. At 3.5 bar, the adsorbed equilibrium amount for CO<sub>2</sub>, CH<sub>4</sub>, and N<sub>2</sub> in BFKY is around 6.42, 1.45, and 0.67 mol kg<sup>-1</sup>, respectively, against 4.48, 1.34, and 0.81 mol kg<sup>-1</sup> in BF4A. Regarding the affinity of adsorption for each component, CO<sub>2</sub> has a much higher affinity than CH<sub>4</sub> and N<sub>2</sub> in both adsorbents. This can be explained due to its large linear quadrupole moment, which leads to a strong interaction with the intracrystalline charge density framework. An important note is that the CO<sub>2</sub> adsorption equilibrium amount is 45% higher on BFKY than BF4A, which can be explained by the higher electric field in the zeolite faujasite type Y framework induced by an increasing number of charged sites present at the surface as compared to the type A framework [3]. However, the CH<sub>4</sub> and N<sub>2</sub> equilibrium of adsorption on both BF4A and BFKY do not present significant differences at the temperature and pressure studied.

Table 2 summarizes the DSL and standard (one-site) Langmuir isotherm parameters obtained from the fitting of the adsorption equilibrium data of CO<sub>2</sub>, CH<sub>4</sub>, and N<sub>2</sub> in the BF4A and BFKY. Figure 1 clearly shows that the DSL and Langmuir models

**Fig. 1** Adsorption equilibrium isotherms of CO<sub>2</sub>, CH<sub>4</sub>, and N<sub>2</sub> at 313 K in binder-free zeolite 4A (open) and KY (closed symbols); Experimental = symbols; numerical = lines

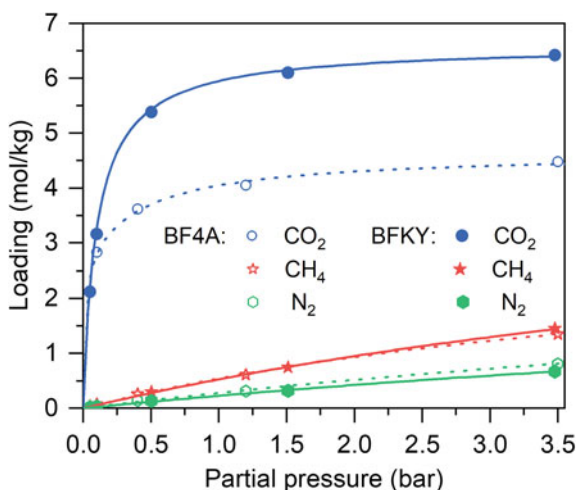


**Table 2** Dual-site and standard Langmuir model parameters for sorption of CO<sub>2</sub>, CH<sub>4</sub>, and N<sub>2</sub> on BF4A and BFKY

Material	Species	$q_m$ (mol·kg <sup>-1</sup> )		$b$ (bar <sup>-1</sup> ) <sup>a</sup>		$(\Delta H_i)$ (kJ·mol <sup>-1</sup> )	
		$q_{m1}$	$q_{m2}$	$b_1$	$b_2$	$(\Delta H_i)_1$	$(\Delta H_i)_2$
BF4A	CO <sub>2</sub>	1.97	2.68	2.44	88.3	-35.6	-38.7
	CH <sub>4</sub>	3.39	–	0.19	–	-18.0	–
	N <sub>2</sub>	3.47	–	0.09	–	-16.2	–
BFKY	CO <sub>2</sub>	3.35	3.25	6.27	16.2	-45.0	-37.4
	CH <sub>4</sub>	4.81	–	0.12	–	-16.9	–
	N <sub>2</sub>	2.98	–	0.08	–	-18.7	–

<sup>a</sup>The reference temperature used is 313.15 K

describe the equilibrium data with good accuracy. The extended DSL (Eqs. 2–8) model was used to predict the multicomponent data in the simulations.

The selectivity of CO<sub>2</sub> over CH<sub>4</sub> and N<sub>2</sub> on BF4A in a typical biogas composition from landfill gas (CO<sub>2</sub>/CH<sub>4</sub>/N<sub>2</sub>:33/52/15 vol.% at 1 bar and 313 K) is equal to 38 and 37, respectively. In the case of BFKY, the selectivity increases to 68 and 66 for CO<sub>2</sub> over CH<sub>4</sub> and N<sub>2</sub>, respectively. These results point out that the BF4A and BFKY can be used to efficiently separate CO<sub>2</sub> from CO<sub>2</sub>/CH<sub>4</sub>/N<sub>2</sub>. These values were calculated by using the extended DSL model and validated experimentally.

It is worth mentioning that raw biogas contains other contaminants such as H<sub>2</sub>O, H<sub>2</sub>S, O<sub>2</sub>, ammonia, and siloxanes whose concentration depends on the source of biogas production [2, 13]. These contaminants can affect significantly the adsorption and separation of CH<sub>4</sub>/CO<sub>2</sub>/N<sub>2</sub>. For example, water can strongly adsorb on both zeolites studied in this work which could reduce their adsorption capacity towards CO<sub>2</sub> leading to a decrease in the overall performance. To use zeolites for biogas upgrading, pretreatment beds (guard beds), for example, for drying the gas stream before feeding the main adsorption column, are necessary to protect it from these contaminants. However, we focus here only on the study of the adsorption dynamics of an ideal mixture of CH<sub>4</sub>/CO<sub>2</sub>/N<sub>2</sub> free of contaminants. For more information about the effect of these contaminants and how they can be removed, detailed information can be found in the work of [2].

### 3.2 Modeling the Breakthrough Data of CH<sub>4</sub>/CO<sub>2</sub>/N<sub>2</sub>

Mathematical modeling of fixed-bed adsorption breakthrough data is a valuable tool to collect adsorption equilibrium data, as well as find the kinetics sorption. The fitting of the experimental breakthrough curves makes it also possible to calculate all model parameters, and thereafter predict the adsorption process performance in a more complex cyclic system, such as: pressure/vacuum swing adsorption; necessary to assure continuous operation in biogas upgrading or any other gas separation process

by adsorption. In this section, the mathematical model developed will be validated and used to predict the dynamics of fixed-bed adsorption by matching the history profiles of the breakthrough curves. As an example, two simulations of a ternary mixture of  $\text{CH}_4/\text{CO}_2/\text{N}_2$  at a certain feed biogas concentration (Table 3) were selected and depicted in Figs. 2 and 3. The experimental conditions and mathematical model parameters are summarized in Table 3.

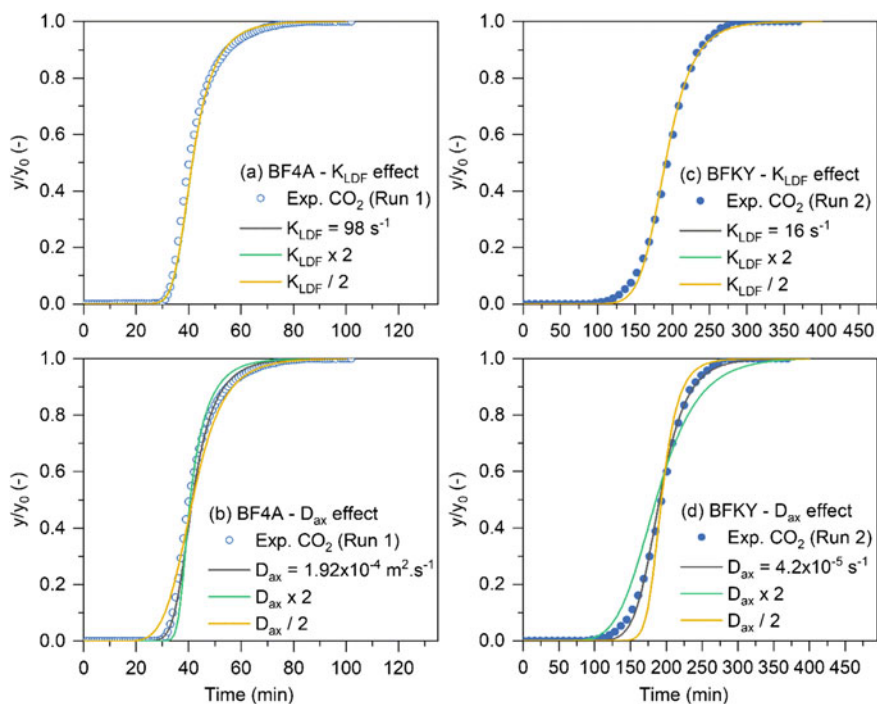
The relative importance of the individual transport mechanisms such as the axial dispersion coefficient ( $D_{ax}$ ) and mass transfer resistance ( $K_{LDF}$ ) was evaluated by performing simulations, where these two parameters were varied to see their effects on the history profile of the breakthrough curves. The  $K_{LDF}$  is the linear driving force coefficient that represents the mass transfer resistance regarding the transport of the solute between the bulk fluid gas phase and the solid phase, and the axial dispersion coefficient ( $D_{ax}$ ) is a resistance arising from fluid mixing and molecular diffusivity in the bulk fluid gas phase.

Figure 2 shows the parametric study performed to evaluate the effect of  $D_{ax}$  and  $K_{LDF}$  in the profile of the breakthrough curves. Figure 2a, c shows that by increasing or decreasing two times the  $K_{LDF}$  and kept  $D_{ax}$  constant, the history profiles of the breakthrough curves are unchanged. On contrary, Fig. 2b, d show that by changing the same values the  $D_{ax}$  and kept  $K_{LDF}$  constant the breakthrough curves are affected. Thus, from this parametric study, we can conclude that experimental breakthrough curves are dependent on the  $D_{ax}$  value. These results agree with the method of moments [7] explored in our previous work [15], where it was shown that axial dispersion mechanisms ( $D_{ax}$ ) are prevailing over the mass transfer resistances ( $K_{LDF}$ ), in the experimental system studied being the numerical model a valuable tool to evaluate such effects.

Figure 3 shows the experimental (symbols) and simulation (lines) ternary breakthrough curve of a mixture  $\text{CO}_2/\text{CH}_4/\text{N}_2$  (20/20/20 vol% balanced with He) in the zeolites (a) BF4A and (b) BFKY. As shown in Fig. 3a-b,  $\text{CO}_2$  is the most retained component due to its high interaction with both zeolite frameworks. In the case of  $\text{CH}_4$  and  $\text{N}_2$ , they break through the column practically at the beginning of the experiments. Thus, we can conclude that both zeolites are excellent adsorbents to separate  $\text{CO}_2$  from a mixture of  $\text{CO}_2/\text{CH}_4/\text{N}_2$ . In general, the numerical simulations represented by the lines in Figs. 2 and 3 describe very well the dynamics of the fixed-bed adsorption system for pure and mixture adsorption. Moreover, the methodology shown here with the validation of the mathematical through laboratory experimentation is the first step and the basis for the rapid scale-up of column testing for the design of cyclic adsorption processes such as PSA/VSA or TSA at an industrial scale regarding biogas upgrading applications.

**Table 3** Experimental conditions and mathematical model parameters

Run	T (K)	P (bar)	Specie	F (mLn/min)	$K_{LDF}$ (1/s)	$D_{ax}$ (m <sup>2</sup> /s)	$K_{ax}$ (W/m/K)	$C_{pg}$ (J/mol/K)	$h_p$ (W/m/K)	$h_w$ (W/m/K)	
1	313	1	CO <sub>2</sub>	28.6	98	$1.94 \times 10^{-4}$	0.25	29.0	190	27	
			He	42.4	-	$1.94 \times 10^{-4}$					
2	313	1	CO <sub>2</sub>	12.8	15.5	$4.17 \times 10^{-5}$	0.13	30.4	37	30	
			N <sub>2</sub>	72.2	16.7	$4.17 \times 10^{-5}$					
3	313	5	CO <sub>2</sub>	117	13	$1.50 \times 10^{-5}$	0.20	18.4	50	137	
			CH <sub>4</sub>	110	5.3	$1.72 \times 10^{-5}$					
			N <sub>2</sub>	121	12.7	$1.70 \times 10^{-5}$					
			He	351	-	$3.62 \times 10^{-5}$					
4	313	1	CO <sub>2</sub>	17.3	29.4	$3.09 \times 10^{-5}$	0.17	29.0	63.4	10.0	
			CH <sub>4</sub>	17.4	42.8	$3.54 \times 10^{-5}$					
			N <sub>2</sub>	17.5	42.8	$3.45 \times 10^{-5}$					
			He	33.7	-	$7.10 \times 10^{-5}$					



**Fig. 2** Effect of changing overall mass transfer coefficient  $K_{LDF}$  (a and c) and axial dispersion  $D_{ax}$  (b and d) on the simulated breakthrough curves of  $CO_2$  at 313 K

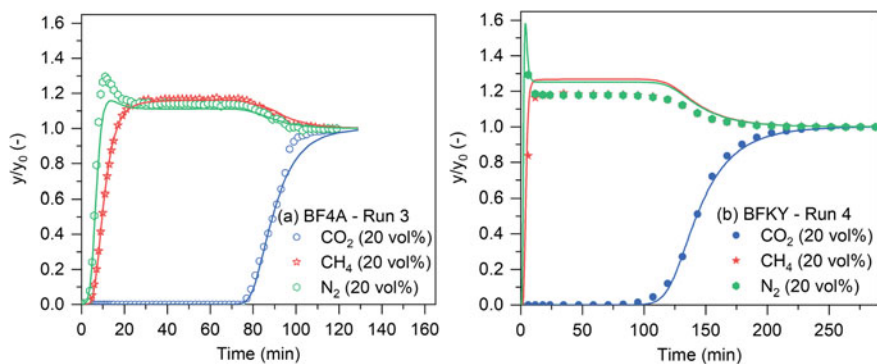


**Fig. 3** Ternary breakthrough curves of  $CO_2/CH_4/N_2$  on a BF4A and b BFKY. Experimental = symbols; Simulation = lines

## 4 Conclusions

In this work, an adsorption package simulator to study the separation of the main components of biogas ( $\text{CO}_2/\text{CH}_4/\text{N}_2$ ) in a fixed bed was developed and validated by fitting experimental single and ternary breakthrough curves on binder-free zeolite 4A and KY. Both zeolites show a significant  $\text{CO}_2$  adsorption capacity with also excellent selectivity over  $\text{CH}_4$  and  $\text{N}_2$ . BFKY adsorbs almost 45% more  $\text{CO}_2$  than BF4A, which is related to the higher electric field presented in the faujasite framework. The mathematical model was validated by predicting the experimental data, at the same time, it gives insights into the prevailing mass transport mechanisms in the fixed bed, being clear that the axial dispersion is the dominant one affecting the history profile of the single and multicomponent breakthrough curves. Overall, the adsorption simulator predicts very well the experimental data shown in this work and, therefore, can be a valuable tool for designing pilot-scale columns and also the development of cyclic adsorption processes, such as PSA, VPSA, and TSA for biogas upgrading.

**Acknowledgements** The authors thank Kristin Gleichmann and Chemiewerk Bad Koestritz GmbH for kindly providing the binder-free beads of zeolite 4A and KY studied in this work. The authors are grateful to the Foundation for Science and Technology (FCT, Portugal) for financial support through national funds FCT/MCTES (PIDDAC) to CIMO (UIDB/00690/2020 and UIDP/00690/2020) and SusTEC (LA/P/0007/2021). Also, the authors thank the Foundation for Science and Technology (FCT, Portugal) under Programme PTDC 2020 \* 3599-PPCDTI \* Engenharia dos Processos Químicos \* project PTDC/EQU-EPQ/0467/2020 and National funding by FCT, Foundation for Science and Technology, through the individual research grant DFA/BD/7925/2020 of Lucas F. A. S. Zafanelli.

## References

1. Aly E et al (2021) Fixed bed adsorption of  $\text{CO}_2$ ,  $\text{CH}_4$ , and  $\text{N}_2$  and their mixtures in potassium-exchanged binder-free beads of Y zeolite. *Ind Eng Chem Res* 60(42):15236–15247. <https://doi.org/10.1021/acs.iecr.1c02261>
2. Awe OW et al (2017) A review of biogas utilisation, purification and upgrading technologies. *Waste Biomass Valorization* 8(2):267–283. <https://doi.org/10.1007/s12649-016-9826-4>
3. Bonenfant D et al (2008) Advances in principal factors influencing carbon dioxide adsorption on zeolites. *Sci Technol Adv Mater* 9(1):013007. <https://doi.org/10.1088/1468-6996/9/1/013007>
4. Canevesi RLS et al (2018) Pressure swing adsorption for biogas upgrading with carbon molecular sieve. *Ind Eng Chem Res* 57(23):8057–8067. <https://doi.org/10.1021/acs.iecr.8b00996>
5. Grande CA (2011) Biogas upgrading by pressure swing adsorption. *Biofuel's Eng Process Technol.* <https://doi.org/10.5772/18428>
6. Grande CA (2012) Advances in pressure swing adsorption for gas separation. *ISRN Chem Eng* 2012:1–13. <https://doi.org/10.5402/2012/982934>
7. Ruthven DM (1984) Principles of adsorption and adsorption processes, 1st edn. Wiley, New York

8. Santos MPS, Grande CA, Rodrigues AE (2011) Pressure swing adsorption for biogas upgrading. Effect of recycling streams in pressure swing adsorption design. *Ind Eng Chem Res* 50(2):974–985. <https://doi.org/10.1021/ie100757u>
9. Schiesser WE, Griffiths GW (2009) A compendium of partial differential equation models. Cambridge University Press, Cambridge. <https://doi.org/10.1017/CBO9780511576270>
10. Schumann K et al (2011) Bindemittelfreie zeolithische Molekularsiebe der Typen LTA und FAU. *Chem-Ing-Tech* 83(12):2237–2243. <https://doi.org/10.1002/cite.201100151>
11. Schumann K et al (2012) Investigation on the pore structure of binderless zeolite 13× shapes. *Microporous Mesoporous Mater* 154:119–123. <https://doi.org/10.1016/j.micromeso.2011.07.015>
12. Shampine LF, Reichelt MW (1997) The MATLAB ODE suite. *SIAM J Sci Comput* 18:1–22
13. Silva J et al (2021) Levels of volatile methylsiloxanes in urban wastewater sludges at various steps of treatment. *Environ Chem Lett* 19(3):2723–2732. <https://doi.org/10.1007/s10311-021-01191-1>
14. Villadsen J, Michael LM (1978) Solution of differential equation models by polynomial approximation. Englewood Cliffs, N. J., Prentice-Hall, New Jersey
15. Zafanelli LFAS et al (2020) Single- and multicomponent fixed bed adsorption of CO<sub>2</sub>, CH<sub>4</sub>, and N<sub>2</sub> in binder-free beads of 4A zeolite. *Ind Eng Chem Res* 59(30):13724–13734. <https://doi.org/10.1021/acs.iecr.0c01911>
16. Zhao Q et al (2019) CO<sub>2</sub> capture using a novel hybrid monolith (H-ZSM5/activated carbon) as adsorbent by combined vacuum and electric swing adsorption (VESA). *Chem Eng J* 358:707–717. <https://doi.org/10.1016/j.cej.2018.09.196>